CREEP-RUPTURE AND FRACTOGRAPHIC ANALYSIS OF STIRLING ENGINE SUPERALLOYS TESTED IN AIR AND 15 MPa HYDROGEN

S. Bhattacharyya* and R. H. Titran**

**IIT Research Institute, Chicago, IL 60616, USA*
***NASA-Lewis Research Center, Cleveland, OH 44135, USA*

ABSTRACT

Effects of high-pressure hydrogen, which is the working fluid in the automotive Stirling engine, on creep-rupture properties of two superalloys were evaluated in specially constructed multispecimen test equipment.

KEYWORDS

High-pressure hydrogen, rupture life, minimum creep rate, elongation, superalloys, temperature-compensated analysis, apparent activation energy, grain boundary voids.

INTRODUCTION

The Department of Energy and NASA-Lewis Research Center have a joint program under way to develop the Stirling engine as an alternative to the automotive internal combustion engine. Advantages of the Stirling engine include the potential for high fuel efficiency, multiple fuel capability, low pollution, and low noise. To achieve these operating characteristics, the Stirling engine will operate at 820°C and use high-pressure H_2 as the working fluid.

The long-term effects of high-pressure hydrogen at high temperature on the properties of high-temperature alloys are unknown. The most critical component in the engine is the heater head, which consists of tubes, cylinders, and regenerator housings. Candidate alloys for these applications must not only meet all the property requirements in air as well as in high-pressure hydrogen, but must also be of low cost to be compatible with automotive application. Six iron-base superalloys were selected for creep-rupture property evaluation over the temperature range of 650°-925°C in air and in 15 MPa H_2, and reports on Stirling engine material studies in air have been issued periodically (Bhattacharyya, 1982, 1984a,b; Stephens, 1981; Misencik, 1980; Witzke, 1980). This paper presents a brief comparative analytical and microstructural evaluation of creep-rupture performance of two iron-base superalloys, one wrought and one cast, in air and 15 MPa hydrogen.

MATERIALS AND EXPERIMENTAL PROCEDURES

The sheet alloy 19-9DL and the cast alloy XF-818 were evaluated; their nominal chemical compositions (in weight percent) are given below.

Alloy	C	Mn	Si	Cr	Ni	Mo	W	Cb	Ti	B	N	Fe
19-9DL	0.30	1.10	0.60	19	9.0	1.25	1.20	0.40	0.30	-	-	Bal
XF-818	0.20	0.15	0.30	18	18	7.5	-	0.40	-	0.70	0.12	Bal

19-9DL was obtained from a commercial supplier in the form of 0.99 mm sheet which was comparable to the wall thickness of the heater head tubes. XF-818 specimens were investment cast by Climax Molybdenum Co. of Ann Arbor, Michigan; the alloy is intended for cylinders and regenerator housings.

Alloy 19-9DL was solution annealed at 1204°C for 10 min and rapidly cooled to room temperature, resulting in a 33 μm grain size and a 50 HRA hardness. XF-818 was used in the as-cast condition and had a hardness almost identical to that of 19-9DL. 19-9DL has an austenitic microstructure with fine second-phase strengthening precipitates, dispersoids, and some inclusions. The cast dendritic structure of XF-818 with carbides and lamellar M_3B_2 eutectic structure is typical of these high-boron alloys.

Details of air test equipment and procedures have been published elsewhere (Bhattacharyya, 1982), while hydrogen test equipment details will be available shortly in the form of a NASA report (Bhattacharyya and others, 1984).

EXPERIMENTAL RESULTS AND ANALYSIS

Basic Data

All air and 15 MPa H_2 creep-rupture data for alloys 19-9DL and XF-818 are given in Tables 1 and 2, respectively. The data can be broadly grouped into two categories: independent (controlled) and dependent (derived). The independent category covers environment (air or 15 MPa H_2), alloy type, temperature, and applied initial stress. The observed data were rupture life (t_r), minimum creep rate ($\dot{\varepsilon}_m$), time to reach 1% creep strain ($t_{0.01}$), and total elongation (ε).

The creep-strain vs. time plots were obtained graphically using a data logging computer storage system for all high-pressure H_2 tests. Sensitive internal transducers were used in all H_2 tests. The similarity between the H_2 and air curves indicates the absence of environmental effects on creep.

Analytical Approach

Of the many different methods of analysis combining stress and temperature (Sherby, 1962; Dorn, 1957; Goldhoff, 1978), the Orowan-Sherby-Dorn (OSD) method given below was used:

$$\ln Y = \ln k + n \ln \sigma + Q/RT \qquad (1)$$

where Y is t_r, $\dot{\varepsilon}_m$, or $t_{0.01}$, σ is the initial stress, k and n are constants, Q is the apparent activation energy, R and T have the known identifications. A linear regression analysis was performed on the data given in Tables 1 and 2, separately for air (Bhattacharyya, 1982) and 15 MPa H_2 (Bhattacharyya and

TABLE 1 Alloy 19-9DL Creep-Rupture Data

Temp. (T), °C	Initial Stress (σ), MPa	Rupture Life (t_r), h	Min. Creep Rate ($\dot{\varepsilon}_m$), s^{-1}	Time to Reach 1% Creep Strain ($t_{0.01}$), h	Total Elongation (ε), %
			Air Tests		
650	414	1.1	4.72E-06	a	18.8
	310	27.9	9.29E-08	1.9	10.1
	276	135.9	3.58E-08	32.0	11.9
705	276	10.9	5.97E-07	0.7	16.9
	172	268.5	5.69E-08	50.0	24.2
	131	1342	1.14E-08	152	12.1
760	193	8.5	1.35E-06	a	30.0
	172	20.2	6.95E-07	2.5	31.0
	138	101	3.22E-07	9.0	37.4
	100	739.1	1.86E-08	89.0	18.8
	86	1687	5.77E-09	300	12.1
815	138	2.8	2.22E-05	a	44.8
	124	14.2	3.33E-06	0.4	33.4
	103	66.4	4.33E-07	4.0	29.2
	83	173.1	1.44E-07	11.0	32.3
	72	324.1	6.03E-08	40.0	25.0
	59	1118	5.72E-09	330	10.1
870	103	1.8	1.89E-05	a	61.6
	83	10.2	5.00E-06	0.4	42.4
	69	38.0	1.60E-06	1.2	36.4
	55	107.9	3.47E-07	8.0	34.3
	41	406.3	3.19E-08	82.0	20.8
	33	799.0	2.00E-08	89.0	
	29	1300	6.94E-09	279	12.3
925	69	4.1	1.58E-05	0.2	47.6
	55	16.3	3.06E-06	0.7	37.1
	35	177.2	1.25E-07	10.5	27.5
			15 MPa H_2 Tests		
705	306	1.7	1.68E-06	a	8.0
	237	28.4	2.29E-07	3.7	15.0
760	163	20.7	4.31E-07	1.7	28.5
	109	304	4.07E-08	24.9	9.3
	88.5	1195	5.32E-09	85.3	7.9
815	93.4	32.1	2.09E-07	7.8	9.4
	72.7	342	3.36E-08	31.1	9.3
	71.3	508	1.81E-08	50.0	9.0
	57.8	1331[b]	9.50E-10	1028	2.9[b]

[a]Time to 1% strain was less than 0.1 h.
[b]Discontinued without failure.

TABLE 2 Alloy XF-818 Creep-Rupture Data

Temp. (T), °C	Initial Stress (σ), MPa	Rupture Life (t_r), h	Min. Creep Rate ($\dot{\varepsilon}_m$), s^{-1}	Time to Reach 1% Creep Strain ($t_{0.01}$), h	Total Elongation (ε), %
			Air Tests		
650	414	143.2	6.72E-08	11.0	7.5
	393	300.8	3.11E-08	17.0	8.0
705	414	3.1	1.60E-06	0.3	6.7
	379	20.9	3.97E-07	3.5	7.2
	331	103.0	9.42E-08	10.5	10.1
	283	541.0	1.52E-08	130	9.9
760	345	2.3	4.12E-06	0.3	8.2
	262	38.4	3.50E-07	4.5	12.7
	221	132.3	1.16E-07	14.0	13.6
	207	261.7	5.67E-08	31.5	12.7
	152	2497	4.58E-09	300	11.4
815	241	4.2	2.77E-06	0.5	13.1
	172	62.5	3.50E-07	5.0	22.3
	138	199.5	8.33E-08	14.5	14.1
	117	1104	1.78E-08	60.0	18.9
	103	3115	4.87E-09	200	23.8
870	172	4.1	5.15E-06	0.4	16.9
	117	58.5	3.64E-07	4.5	20.6
	97	194.0	9.00E-08	14.0	19.0
	63	2198	6.78E-09	205	12.9
925	103	11.8	2.11E-06	0.8	25.2
	69	128.5	1.46E-07	15.0	23.1
	55	316.4	5.36E-08	20.0	18.4
			15 MPa H_2 Tests		
705	396	6.4	6.94E-07	1.1	5.0
	395	15.0	a	a	6.0
760	216	182	5.44E-08	27.5	10.4
	166	1492[b]	5.99E-09	194	6.6[b]
815	176	56.7	1.17E-07	7.8	10.3
	133	275	4.00E-08	39.0	14.2
	131	200	5.51E-08	13.0	10.1
	118	1091	9.70E-09	200	16.2
870	93.6	221	5.90E-08	38.0	15.4

[a]Transducer malfunctioned.
[b]Discontinued without failure.

others, 1984) environments. The analysis determined n, the stress exponent; Q, the apparent activation energy; k, the fitting constant; and R^2, the multiple correlation coefficient. Because the amount of air data was twice as large as hydrogen data, the multiple correlation coefficient, R^2, for air analysis was often times higher.

The OSD relationship was rearranged in the following manner:

$$\ln Y - Q/RT = \ln k + n \ln \sigma \qquad (2)$$

and plotted in Figs. 1 and 2 for rupture life vs. stress for 19-9DL and XF-818, respectively. Similar graphical relationships, not shown, were obtained for $\dot{\varepsilon}_m$ and $t_{0.01}$ vs. stress.

Rupture Life Analysis

The stress slope (n) and the apparent activation energies (Q) for rupture life in the two environments were as follows:

Alloy	Environment	No. of Data	R^2	ln k	Stress Slope (n)	Apparent Activation Energy (Q), kJ/mole
19-9DL	Air	19	0.975	-17.6	-6.44	461
	15 MPa H_2	8	0.974	-18.1	-7.89	522
XF-818	Air	14	0.991	-13.2	-7.52	505
	15 MPa H_2	7	0.918	1.91	-7.09	349

Minimum Creep Rate Analysis

A similar analysis for the minimum creep rate showed the following:

Alloy	Environment	No. of Data	R^2	ln k	Stress Slope (n)	Apparent Activation Energy (Q), kJ/mole
19-9DL	Air	19	0.948	15.2	7.38	-573
	15 MPa H_2	9	0.941	9.93	8.10	-564
XF-818	Air	14	0.990	6.85	7.47	-545
	15 MPa H_2	7	0.866	-5.84	7.60	-441

The stress slope values tend to indicate that in 19-9DL both rupture life and minimum creep rate become more sharply dependent on small stress changes. In XF-818, the dependence on stress is not significantly affected by the environment. The apparent activation energy values do not provide a clear trend. As to rupture life, 19-9DL appears to become a more creep resistant material with an increasing Q while the opposite is noted for XF-818. As to minimum creep rate, there appears to be no environment effect with 19-9DL, whereas Q becomes less negative for XF-818 under 15 MPa H_2.

Total Elongation

Specimen elongations in the two environments shown in Fig. 3 indicate a similar H_2 effect in decreasing elongation at rupture in both the alloys.

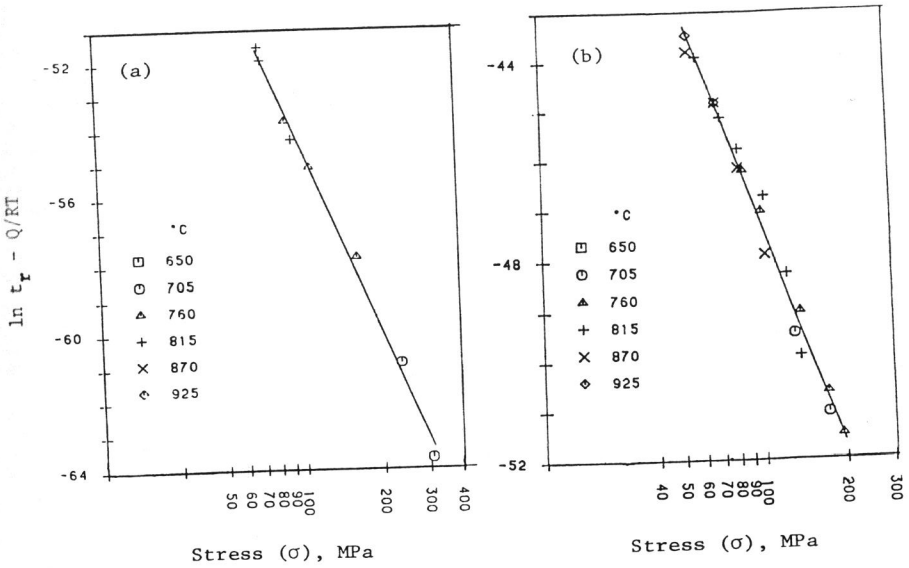

Fig. 1. Effect of environment on temperature-compensated rupture life for 19-9DL alloy. (a) 15 MPa H_2, (b) air.

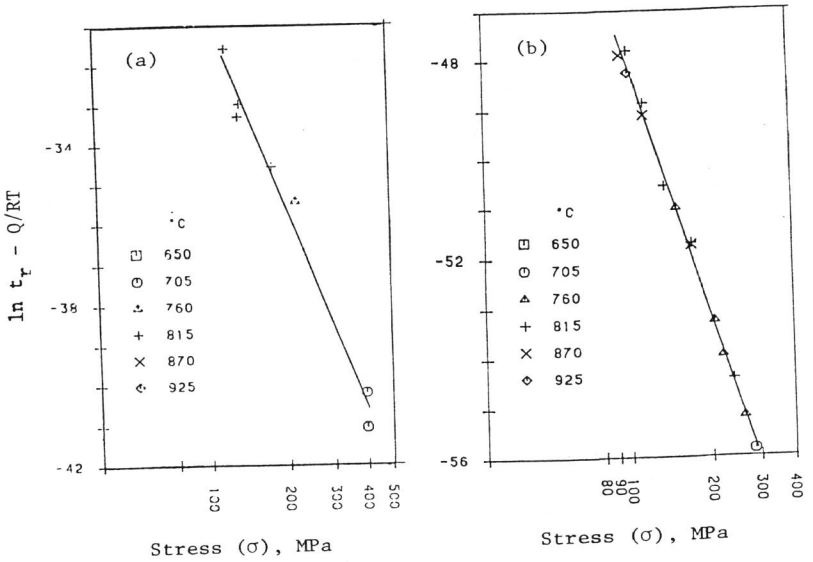

Fig. 2. Effect of environment on temperature-compensated rupture life for XF-818 alloy. (a) 15 MPa H_2, (b) air.

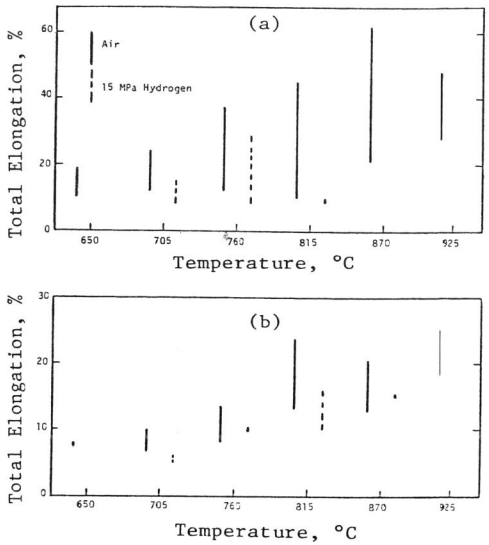

Fig. 3. Effect of environment on total elongation. (a) 19-9DL, (b) XF-818.

3500-h Rupture Life Stress

The MOD 1A Stirling automotive engine design criteria (Cornwall, 1981) indicate that the effective engine life should be taken to be 3500 h of running time. Based on the temperature-compensated analytical data, stresses for 3500-h rupture lives were estimated, indicating no significant effect of H_2 on rupture life. For example, in 19-9DL the stresses for 870°C/3500-h life in air and 15 MPa H_2 were 34 and 38 MPa, respectively, and for XF-818, the corresponding values for 775°C/3500-h life were 130 and 118 MPa, respectively. The design stresses for 19-9DL and XF-818 were 28 MPa at 870°C and 119 MPa at 775°C, respectively; XF-818 appears to be marginally inadequate in H_2 environment and needs further alloy development, which is now under way.

FRACTOGRAPHY AND MICROSTRUCTURE ANALYSIS

Examination of fracture surfaces indicated no definite crack initiation sites, and multiple cracks were observed to be initiated from the surface leading to rupture. Sheet specimens showed many more such cracks close to the fracture surface than the cast specimens. Almost all the fractures appeared rough, rugged, and granular. The main fracture mode was decohesive rupture associated initimately with dimple rupture. Detailed fractography of all six alloys tested in air has been published (Bhattacharyya, 1982).

19-9DL

Typical specimen fractographs are shown in Fig. 4. Fracture surfaces in H_2 (Figs. 4b) were similar in appearance to those tested in air (Fig. 4a), and were extremely rough with origins at multiple locations. The overloaded middle region reveals dimple rupture with inclusions rich in chromium located inside the dimples (Fig. 4c). The H_2 test fracture (Fig. 4b) reveals over two-thirds of the region covered with fine dimples (Fig. 4d).

Fractured specimens, polished to mid-thickness, indicated that fracture was extensive through the section. Large angular grain boundary (gb) carbides observed appeared to be more continuous at the fracture surface than those away from the edge, and because of their continuity even in areas away from the fracture edge (Fig. 4e) oxides were noted at the gb's. H_2-tested specimens had fractures close to both edges as well as in the interior with evidence of voids along gb's (Fig. 4f) which coalesced and led to fracture.

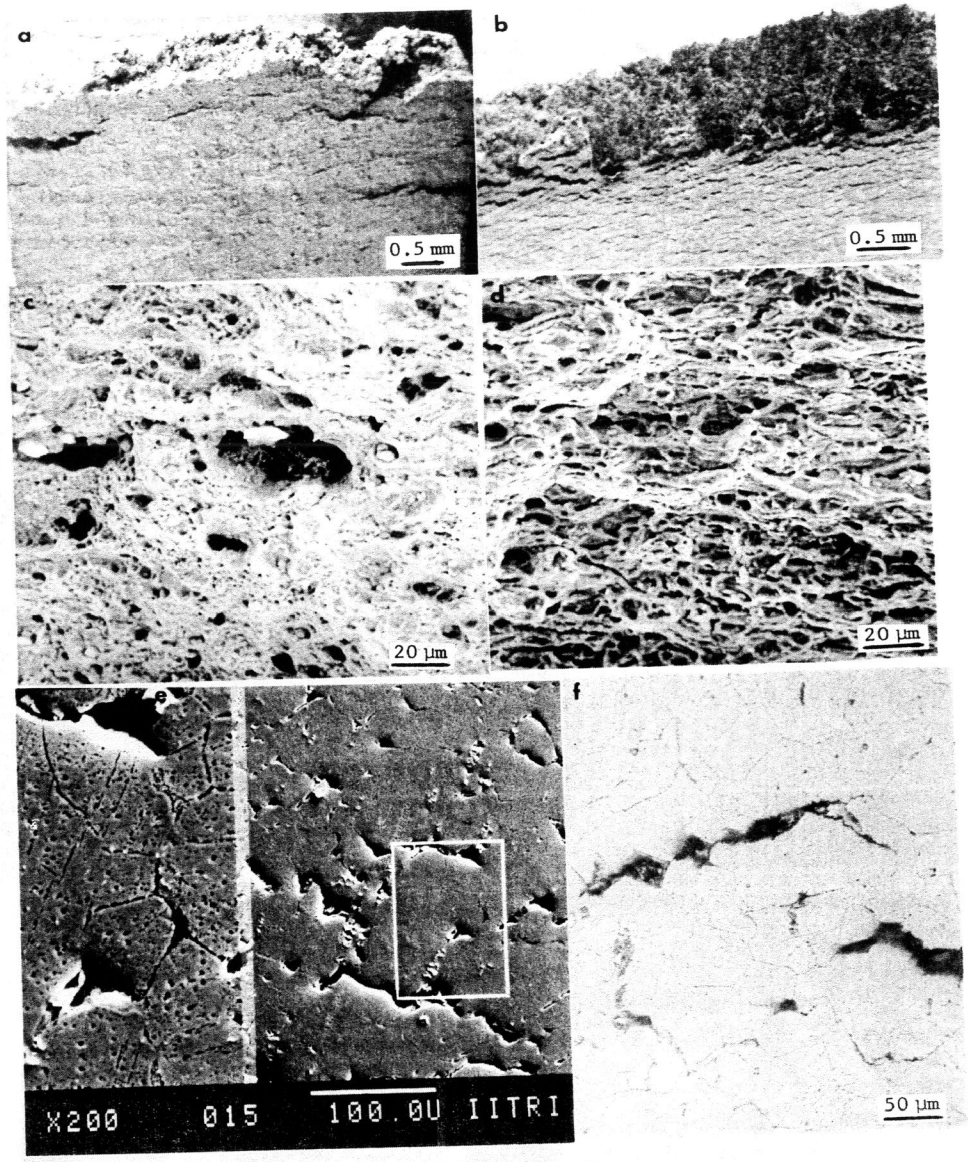

Fig. 4. 19-9DL: SEM macro- and micrographs of fracture surfaces. (a,c,e) Tested in air; (b,d,f) tested in 15 MPa H_2. (a) 870°C/29 MPa, (b,d) 705°C/237 MPa, (c) 705°C/131 MPa, (e) 815°C/59 MPa, (f) 760°C/88.5 MPa.

XF-818

Air-tested specimen fractures were rough with relatively smooth facets intermixed with rugged areas. Columnar fracture along dendritic orientation can be seen in Fig. 5a. Dimples, absent at lower temperatures, covered the columnar dendrites at the higher temperatures.

Hydrogen fracture surfaces (Fig. 5b) indicated different degrees of ductility along with dimple rupture (Fig. 5c). Fracture followed an interdendritic path with dendrite areas near the fracture appearing to be oriented more perpendicularly to the fracture edge. At higher temperatures, fracture had also occurred by interdendritic rupture with cracks in the eutectic structure (Fig. 5d). Interdendritic phases consisted of a lamellar boride phase alternating with austenite. The lamellar phase between the arms had a heavy concentration of molybdenum with localized concentration of boron.

The structural analysis indicated that the predominant mode of rupture did not alter due to environment effect. However, more subtle effects have occurred as evidenced by a decrease in total elongation in H_2. The sliding of grains sets up stress concentration at the grain junctions and at the various irregularities (second phases, porosity, etc.) along the grain boundaries. Local decohesion and cavity formation lead on to crack initiation and rupture. H_2 accumulation in these cracks and voids may accelerate crack propagation and decrease overall ductility.

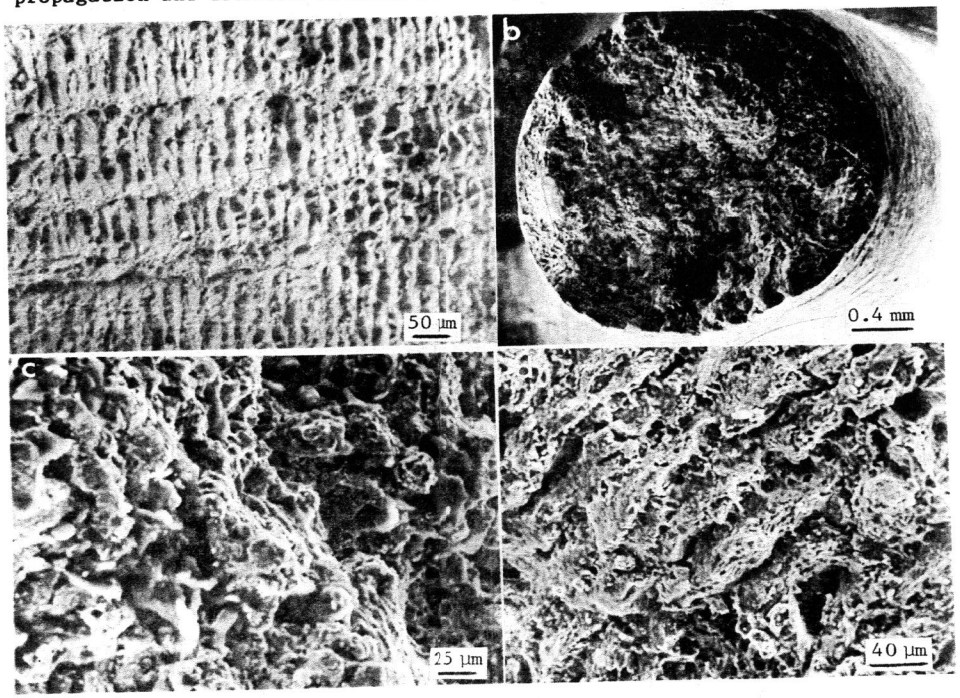

Fig. 5. XF-818: SEM macro- and micrographs of fracture surfaces. (a) Tested in air; (b-d) tested in 15 MPa H_2. (a) 815°C/138 MPa, (b,c) 760°C/216 MPa, (d) 815°C/176 MPa.

SUMMARY AND CONCLUSIONS

Wrought alloy 19-9DL and cast alloy XF-818 intended for the Stirling engine were tested in air and 15 MPa H_2. The rupture life, minimum creep rate, time to 1% creep strain, and total elongation were analyzed, and fracture surfaces were evaluated. The analysis indicated the following:

- At the MOD 1A engine maximum operating temperature of 870°C and 28 MPa design stress level, the tube alloy 19-9DL remained adequate in 15 MPa H_2. Alloy XF-818 with a design stress of 119 MPa at 775°C became marginally inadequate indicating the need for further alloy development.
- High-pressure hydrogen had a significant effect in reducing rupture ductility for both 19-9DL and XF-818.
- No effect of 15 MPa H_2 (as compared to air) was noted on fracture modes or on structure and grain boundaries.

ACKNOWLEDGEMENTS

This study was sponsored under Contract DEN3-217 by NASA-Lewis Research Center, Cleveland, OH, for the U.S. Department of Energy, Office of Transportation Programs. We thank W. R. Witzke, and J. R. Stephens of NASA-Lewis for their help. At IITRI, contributions were made by C. Hales, C. J. Moore, H. Nichols, S. C. Agarwal, and M. Dimenn.

REFERENCES

Bhattacharyya, S. (1982). Creep-rupture behavior of six candidate Stirling engine iron-base superalloys in high pressure hydrogen. Volume 1 - Air creep-rupture behavior. NASA CR-168071.

Bhattacharyya, S. (1984a). Creep-rupture behavior of six candidate Stirling engine superalloys tested in air. J. of Mater. Technol., ASME. Accepted for publication.

Bhattacharyya, S. (1984b). Creep-rupture and fractographic analysis of candidate Stirling engine superalloys in air. J. Mater. Energy Syst., ASM. Accepted for publication.

Bhattacharyya, S., W. Peterman, and C. Hales (1984). Creep-rupture behavior of Stirling engine iron superalloys in high-pressure hydrogen, Volume 2 - 15 MPa H_2 behavior. NASA CR- (in preparation).

Cornwall, J. (1981). Tentative heater design stress criteria in automotive applications. United Stirling AB, Sweden, Report No. 81-0023.

Dorn, J. E. (1957). Spectrum of activation energies for creep. In Creep and Recovery, ASM, Metals Park, Ohio, pp. 255-283.

Goldhoff, R. M. (1978). The evaluation of elevated temperature creep and rupture strength data: an historical perspective. In G. V. Smith (ed.), Characterization of Materials for Service at Elevated Temperatures, Publ. No. MPC-7. ASME, New York, pp. 247-265.

Misencik, J. A. (1980). Evaluation of candidate stirling engine heater tube alloys for 1000 hours at 760°C. NASA TM-81578.

Sherby, O. D. (1962). Acta Met., 10, No. 2, 135-147.

Stephens, J. R. (1981). Conf. Proc. on Environment Degradation of Engineering Materials in Hydrogen, Sept.21-23, Virginia Polytechnic Institute, Blacksburg, Virginia, pp. 123-132.

Witzke, W.R., and J.R. Stephens (1980). Creep-rupture behavior of seven iron-base alloys after long-term aging at 760°C in low pressure hydrogen. NASA-TM-81534.